Proc. Natl. Acad. Sci. USA
Vol. 83, pp. 3791–3795, June 1986
Biophysics

Small-angle neutron scattering studies of chlorophyll micelles: Models for bacterial antenna chlorophyll

(photosynthesis/energy transfer/chlorosomes)

D. L. WORCESTER, T. J. MICHALSKI, AND J. J. KATZ

Chemistry Division and Pulsed Neutron Source, Argonne National Laboratory, Argonne, IL 60439

Contributed by J. J. Katz, January 7, 1986

ABSTRACT **Micelles of hydrated chlorophyll a (P740), bacteriochlorophyll a (P865), bacteriochlorophyll c (P750), and pheophytin a prepared in organic media have been studied by small-angle neutron scattering to determine their shape, size, and mass per unit length. All of the micelles are hollow cylinders of well-defined size. The P740 and P750 cylinders are essentially monolayers of macrocycles crosslinked by water, probably in an arrangement similar to that of crystals of chlorophyll derivatives. The P865 micelle is more nearly a bilayer of macrocycles. We show that the curvature necessary to form cylinders probably results from intrinsic curvature of the five-coordinated chlorophyll macrocycle. Studies of P740 micelle formation and the disaggregating effects of another nucleophile (pyridine) are described. As the P750 micelles are nearly identical in size and optical spectra to the rod-shaped structures observed in chlorosomes, and the P865 micelles have optical properties very similar to the *in vivo* properties of the long-wavelength antenna of purple photosynthetic bacteria, we propose that features of the hydrated cylindrical micelles of these chlorophylls provide good models for antenna chlorophyll in photosynthetic bacteria.**

Many artificial chlorophyll systems (colloidal dispersions, films, monolayers, adsorbates) are of interest because their visible absorption maxima are red-shifted relative to the corresponding monomeric chlorophyll, a feature that is also characteristic of chlorophylls *in vivo* (1). Of particular importance are the chlorophyll/water micelles formed in nonpolar organic solvents. Chlorophyll a/water micelles so formed are red-shifted from 660 nm (monomer) to 740 nm and are photoactive in red light (2). Bacteriochlorophyll a/water micelles (P865) have red-shifted optical spectra that strongly resemble those of intact purple photosynthetic bacteria (3). As no direct structural information on these systems exists, we have undertaken a small-angle neutron-scattering study of chlorophyll/water micelles in organic media, using the Intense Pulsed Neutron Source (IPNS) at the Argonne National Laboratory and the High Flux Reactor of the Institut Laue-Langevin, Grenoble, France.

MATERIALS AND METHODS

Materials. Chlorophyll a (Chl*a*), bacteriochlorophyll a (Bchl*a*), *Chlorobium* chlorophyll (Bchl*c*), and pheophytin a (Pheo*a*) were prepared by literature methods (4). Purity was established by HPLC and by californium-252 plasma desorption mass spectroscopy (5). Deuterated solvents (Aldrich) contained <1% ^1H.

Chlorophyll/water micelles were prepared by addition of microliter amounts of ^1H_2O or ^2H_2O to previously dried chlorophyll dissolved (≈10 mg/ml) in a nonpolar solvent. Mild sonication (30 sec) was used to disperse the water. Rigorous drying of the chlorophylls and the solvents (6) before hydration was necessary as the structures formed from undried or partially dried starting materials can vary. Samples for small-angle neutron scattering were sealed in 2- to 5-mm-thick quartz cells.

Neutron Scattering. Chlorophylls of natural isotopic composition were studied in deuterated solvents to enhance the scattering intensity in much the same way neutrons have been used to study synthetic polymers and micellar structures (7). Measurements were mostly made on the small-angle scattering instrument of the Argonne IPNS. Neutrons produced in pulses by spallation processes from 450 MeV protons were moderated and passed through collimators to produce a beam of small angular divergence. The scattered neutrons were detected in a 17 × 17 cm^2 He^3 multidetector, and the wavelengths were established by time-of-flight. The incident neutrons were monitored as a function of wavelength to normalize scattering intensities. Sample scattering data were corrected by subtracting the scattering from quartz cells containing solvent only. The corrected scattering data were further evaluated to obtain the scattered intensity as a function of $Q = 4\pi \sin\theta/\lambda$, where θ is half the scattering angle and λ is the wavelength.

During these experiments the IPNS instrument was much improved by installation of colder moderators to enhance production of long-wavelength neutrons. The instrument now has a solid-methane moderator at 12 K that allows use of neutrons from 0.05 to 1.4 nm wavelengths. Scattering from several chlorophyll/water samples was measured at IPNS in the Q range 0.1–2 nm^{-1} during early experiments. For these samples, scattering at smaller values of Q (to 3×10^{-2} nm^{-1}) was measured using the instruments D-11 and D-17 at the Institut Laue-Langevin, Grenoble, France. In the most recent experiments reported here, the IPNS solid-methane moderator permitted measurements down to Q values of 4×10^{-2} nm^{-1}.

RESULTS

Scattering Data. Scattering data for several chlorophyll/water micelles are shown in Fig. 1. A striking feature of the data is the series of secondary maxima. The clear minima between the maxima indicate that the aggregates are substantially homogeneous in size and shape. Of possible structural types (spherical micelles, cylinders, or flat sheets), the scattering patterns strongly indicate cylindrical micelles. At small Q, the best linearity was obtained for Guinier plots of the cylindrical type, in which $\ln[Q \cdot I(Q)]$ is plotted against Q^2 (Fig. 2). Cross-sectional radii of gyration obtained for chlorophyll micelles are listed in Table 1.

Radial density distributions were calculated by Fourier–

The publication costs of this article were defrayed in part by page charge payment. This article must therefore be hereby marked "*advertisement*" in accordance with 18 U.S.C. §1734 solely to indicate this fact.

Abbreviations: Chl*a*, chlorophyll a; Bchl*a* or -*c*, bacteriochlorophyll a or c; Pheo*a*, pheophytin a.

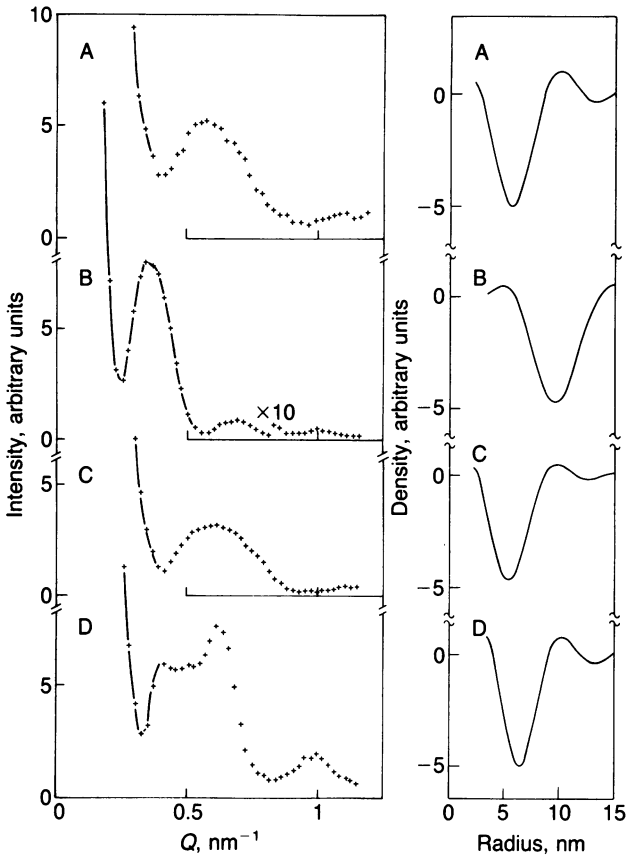

FIG. 1. Neutron scattering data (*Left*) and radial density profiles (*Right*) of Chl*a*/^2H_2O (*A*), Bchl*a*/^2H_2O (*B*), Bchl*c*/^2H_2O (*C*), and Pheo*a*/^2H_2O (*D*).

Bessel transformation with alternating plus and minus signs for the amplitudes of successive secondary maxima:

$$\rho(r) = \int_0^\infty (\pm)\, Q^{3/2} I^{1/2}(Q) J_0(Qr) dQ,$$

where $J_0(Qr)$ is the zero-order Bessel function of the first kind. The density profiles so obtained are shown in Fig. 1 beside their respective scattering data. The chlorophylls are located at radii where the densities are negative because the chlorophylls have smaller scattering length densities than the deuterated solvents.

The mass per unit length of the micelles was determined from cylindrical-type Guinier plots extrapolated to $Q = 0$. The ratio of this intensity to the intensity of scattering from water is given by

$$\frac{(Q \cdot I)_{Q=0}}{I_{H_2O}} = \frac{4\pi^2}{(1-T)} T_s D C \left(N \frac{\Sigma b}{M} - \rho_s \bar{\nu} \right)^2 \frac{\mu}{N},$$

where μ is the mass/unit length, D is the sample thickness,

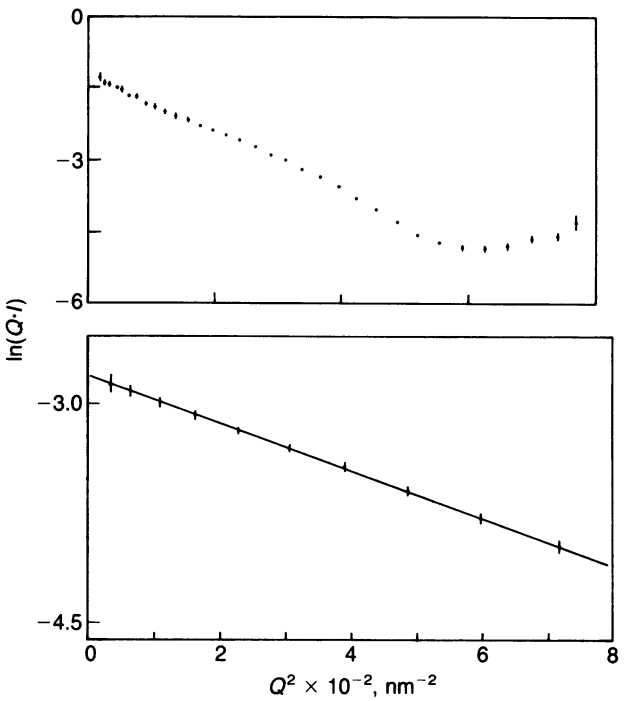

FIG. 2. Cylindrical-type Guinier plots of neutron scattering data for determination of cross-sectional radii of gyration (R_c). The slope at small Q is $-R_c^2/2$. (*Upper*) Bchl*a*/^2H_2O (sample of Fig. 1*B*) measured on the instrument D-11 (10.5 m from sample to detector) of the Institut Laue-Langevin. (*Lower*) Chl*a*/^2H_2O (sample of Fig. 1*A*) measured on the IPNS small-angle instrument (1.5 m from sample to detector) after installation of the solid-methane moderator.

T_s and T are the sample and H_2O transmissions, M is the chlorophyll mass, C is the concentration, Σb is the sum of the neutron scattering lengths of the chlorophyll atoms, ρ_s is the solvent scattering density, $\bar{\nu}$ is the partial specific volume of the hydrated chlorophylls, and N is Avogadro's number. The partial specific volume used was that given for Chl*a* P740 microcrystals (0.92 cm^3/g) (9). Mass/unit length values and related data for the chlorophyll micelles are given in Table 1.

Micelle Formation. On hydration, Chl*a* gave micelles whose diameter was independent of the water content, whereas Bchl*a* gave micelles of increasing diameter with increasing amounts of water, up to a maximum diameter of 40 nm. These Bchl*a* micelles made with ^1H_2O gave neutron scattering intensities uniformly enhanced by 15–20% compared to the same starting material hydrated with ^2H_2O. This increase corresponds to 5–6 water molecules per Bchl*a* molecule in the most highly hydrated micelles. In contrast, Bchl*c* always gave micelles similar to those of Chl*a*, even when no water was added to the dry system.

We also made a small-angle neutron scattering study of Chl*a* micelle formation. Dry Chl*a* in octane forms oligomers,

Table 1. Structural parameters for chlorophyll/water micelles

	Solvent*	Conc.,† mg/ml	λ_{max}, nm	R_c, nm	Profile width, nm	Mass/length,† daltons/nm	Molecules‡ per nm²
Chl*a*	0	2.2	740	5.7 ± 0.05	3.4	37.3	1.16
Bchl*a*	25	7.3	865	10.5 ± 0.1	4.2	112.0	1.86
Bchl*c*	50	9.8	750	5.9 ± 0.05	3.6	17.4	0.59
Pheo*a*	15	12.8	—	6.8 ± 0.1	3.0	13.0	0.35

*Percent (by volume) perdeuterated toluene in perdeuterated octane.

†The concentrations are the chlorophyll content of the samples, but not all was incorporated into micelles. Some monomeric chlorophyll and fine precipitates were also often present, especially for the Bchl*c* and Pheo*a* samples. Consequently, the mass/unit length values are lower limits.

‡These values for the surface densities of the chlorophylls are the mass/unit length values divided by $2\pi R_c$ and the molecular mass. For comparison, the value for two-dimensional sheets of ethyl chlorophyllide a·$2H_2O$ is 1.47 molecules per nm² (8).

$(Chla)_n$, whose size depends on the Chl*a* concentration. At 10 mg of chlorophyll per ml, we observed scattering intensity corresponding to about 20 Chl*a* molecules per oligomer. These oligomers absorbed maximally at 680 nm. Upon addition of very small amounts of water (<<1 molecule per Chl*a*), the oligomer size increased markedly and the absorption maximum shifted to 715 nm. The viscosity of the system also increased and became sensitive to temperature and agitation. A system containing large oligomers at a Chl*a* concentration of 20 mg/ml was fluid at 40°C and became a solid thixotropic gel at 20°C that could be liquified by agitation. Upon further addition of water, P740 formed, the viscosity of the system dropped sharply, and the neutron scattering of Fig. 1 was obtained. The neutron scattering from the P740 micelles was essentially independent of temperature from 6° to 60°C.

Disaggregation of Micelles. We examined the effect of a strong nucleophile on the Chl*a* micelles to obtain some idea of their susceptibility to nucleophiles that might be encountered *in vivo*. The neutron scattering of Fig. 1*A* was unchanged during successive additions of pyridine to a pyridine/Chl*a* ratio of 8:1. A slow loss of intensity in the secondary maximum occurred on continued addition of pyridine, until it was absent at a ratio of 16:1. This change was accompanied, at small Q, by conversion of the $1/Q$ scattering characteristic of cylinders to a $1/Q^2$ scattering characteristic of thin sheets. This $1/Q^2$ scattering persisted, but with decreasing intensity, during 7 hr of successive additions of pyridine (to 50 pyridine molecules per Chl*a*) and for 5 hr of measurements at this ratio. After an additional 10 hr the scattering was much reduced and was not $1/Q^2$. Thirty hours with a 50:1 excess of pyridine were required to convert the micelle to monomeric chlorophyll. Clearly, the micelle is not easily disrupted by extra nucleophiles at concentrations likely to prevail in photosynthetic organisms.

DISCUSSION

Micelle Structures and Models. The neutron scattering results show that the P740 micelle consists of Chl*a* molecules with interacting, hydrated macrocycles forming a cylindrical shell at about 5.7 nm radius. The structure is tube-like, with solvent in the central cavity of the cylinder and at radii greater than 8.2 nm. The linearity of the Guinier-type plots at small Q indicates that the cylinders are at least 200 nm long and probably longer. Earlier indications of cylindrical chlorophyll structures are electron micrographs taken in 1954 of Chl*a*/water P740 (then known as "microcrystalline" chlorophyll and not clearly known to contain water) that show tiny cylinders formed from rolled sheets (10), and a freeze–fracture electron microscopy study of Chl*a*/water adducts in hexadecane (11).

Structural parameters obtained from the neutron scattering data are the mean radius and width of the shell and the mass/unit length. The small-angle neutron scattering data are too limited to provide detailed arrangements of the chlorophyll macrocycles, but x-ray crystal structures for chlorophyll derivatives provide valuable guidelines for specific models. From the crystal structures of ethylchlorophyllide a·$2H_2O$ and other derivatives of Chl*a* and Chl*b* (8, 12), it is possible to suggest some basic features of the coordination and hydrogen-bonding interactions in the micelles. In the crystal structures, a molecule of water is coordinated to the central magnesium atom and hydrogen-bonded to the ring V keto C=O function of another chlorophyll molecule. Repetition of this interaction forms, in nearly all known crystal structures of chlorophyll-like compounds, a chain of macrocycles in which rings I and III are partially overlapped and in such close proximity that significant π–π interaction results, thus accounting for the observed optical red shifts (13). Similar molecular arrangements are found in crystals of Mg-free chlorophyll derivatives (14–16), indicating that π–π overlap contributes appreciably to stabilizing the chain of macrocycles (17).

In several crystal structures, additional water molecules crosslink the primary chains into two-dimensional sheets. In ethyl and methyl chlorophyllide a·$2H_2O$, the crosslinking is between the carbomethoxy groups in one primary chain and the ester C=O of the phytyl groups in an adjoining chain. It has been suggested that two-dimensional sheets could also be formed with only the Mg-coordinated water molecule present, because a small change in the conformation of the propionic acid side-chain allows direct hydrogen-bonding between the propionic ester C=O and the water coordinated to Mg in an adjoining chain (18). A model for the P740 Chl*a*/water micelle based on the small-angle neutron scattering data and crystal structure considerations is shown in Fig. 3.

Two main possibilities for the orientation of the primary chains in the cylinders are (*i*) chains parallel to the cylinder axis or (*ii*) chains oriented around the circumference of the cylinder as closed rings or a shallow helix. Our studies indicate that the Chl*a* micelles are formed from long linear chains that crosslink in a shallow helix to form the cylinders. Whether this mode of formation also applies to Bchl*a* and -*c* is not yet known.

A basic feature of chlorophyll molecular structure may be responsible for the chain curvature required for cylinder formation. A "best set" of atomic coordinates for hydrated chlorophyll derivatives (19) shows that with a water molecule coordinated to Mg, the Mg atom is 0.04 nm out of the average plane of the macrocycle, and there is substantial tilt of the pyrrole rings. Thus, the macrocycle is bowl-shaped rather than planar, and the normals to rings I and III form an angle of about 7°, a feature also found in a monohydrated Mg–phthalocyanin complex (20). Any tendency of the π–π interaction to form parallel overlapping pyrrole rings therefore results in a chain that is curved rather than straight. This 7° angle per macrocycle, together with the 0.89 nm chain repeat found for ethyl chlorophyllide a·$2H_2O$, would form a ring with a radius of 7.28 nm. Larger curvature in the chlorophyll macrocycle, as might easily be the case for a macrocycle not subject to the constraints of crystal forces, together with a tilt of the macrocycles with respect to the cylinder axis, could shorten the radius of curvature to the value of 5.7 nm observed for the P740 micelles. The curvature of the principal chain could also result from the two points of interaction having different distances between the macrocycles. The hydrogen bonding of the ring V keto C=O function to the Mg-coordinated water molecule probably establishes a greater local distance between macrocycles than the π–π interaction between rings I and III. This feature is possibly involved in the formation of the Pheo*a* micelles.

Tilt of the macrocycles relative to the cylinder axis is required for crosslinking between primary chains. The tilt of the macrocycles may also be implicated in our failure to observe magnetic orientation of the cylinders in a 1.5 T magnetic field (by neutron scattering at 2–5% sensitivity). The chlorophyll macrocycle has a very high diamagnetic anisotropy, and a cylinder of n chlorophyll molecules will have a total diamagnetic anisotropy given by

$$\Delta\chi = n\Delta K\,(1 - 3\cos^2\phi)/2,$$

where ΔK is the molecular anisotropy, and ϕ is the tilt angle between the normal to the macrocycle and the cylinder axis (21). The cylinder would have a large diamagnetic anisotropy for $\phi = 90°$, but would have only a very small diamagnetic anisotropy if ϕ were near the "magic angle" of 55°. In the crystal structures, the normals to the macrocycles are tilted

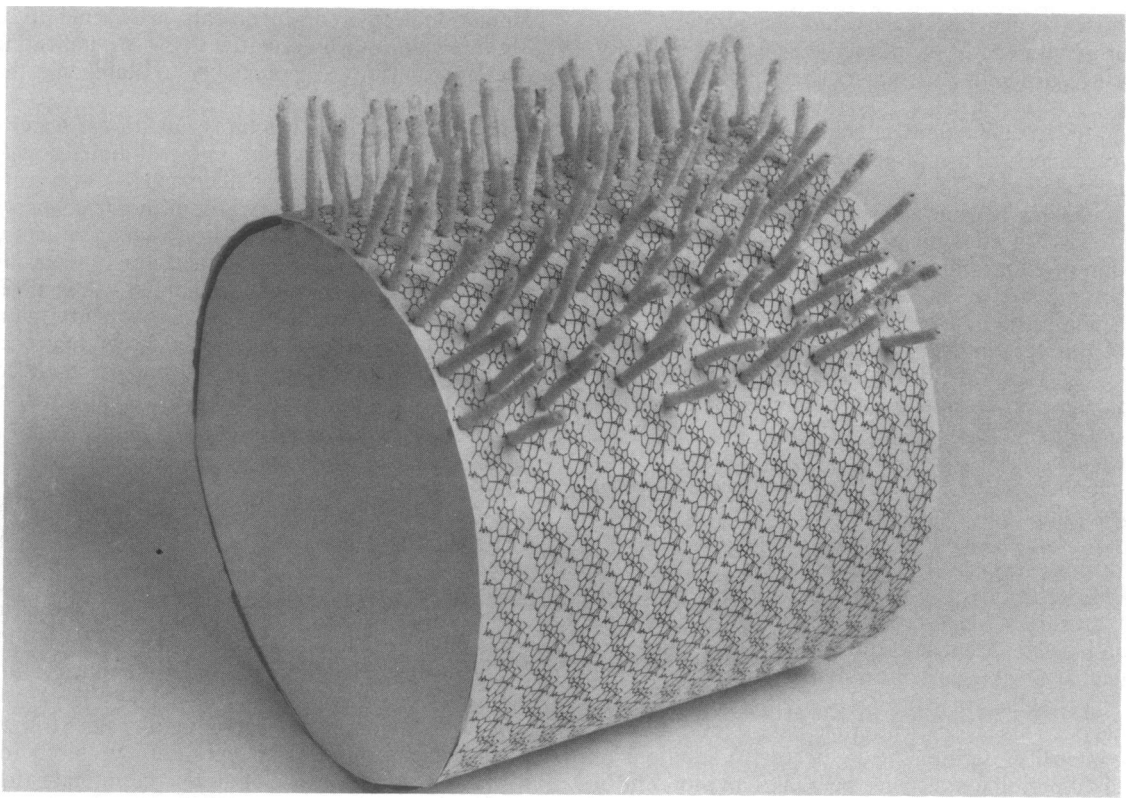

FIG. 3. Model of a short section of the Chl*a*/water cylindrical micelle. The surface is formed by a monolayer of chlorophyll macrocycles interacting as found in crystals of chlorophyll derivatives. Approximately 36 Chl*a* macrocycles form the circumference of the cylinder at a radius of 5.5 nm, arranged in a shallow helix or closed rings (the latter is shown here). The phytyl groups are shown extended here but are probably in disordered conformations in the micelles. Only some of the phytyl chains are shown in order to display the macrocycle network. The model is approximately to scale, so that the regions occupied by the phytyl chains also contain much solvent.

to the sheets by 35°. Another explanation for the lack of magnetic orientation is that the cylinders we prepared are so long that they interfere with each other and cannot be rotated by the magnetic field.

The hydrated micelles from Chl*a*, Bchl*c*, and Bchl*a* are very similar in shape and neutron scattering density distribution but differ in size and in mass per unit length. We suggest that all these micelles are derived from similar principal chains of macrocycles and two-dimensional sheets but that the precise molecular arrangements and assembly processes differ in detail. Differences in the molecular arrangements are expected from the differences in the molecular structures of the chlorophylls. Whereas in Chl*a* the ring V keto C=O function is the most important donor function, Bchl*c* contains in addition a hydroxyethyl group, $CH_3CH(OH)$—, and Bchl*a* an acetyl C=O group. These groups are located symmetrically across the macrocycle from the ring V keto group and are good donors and hydrogen-bonding partners. The main constraint these donors experience is the steric interference of the ring V carbomethoxy group (not present in Bchl*c*). Probably the most important difference between the lattices is that all the Mg atoms in the Chl*a* micelle carry a molecule of coordinated water hydrogen-bonded to a ring V keto group, whereas micelles of Bchl*a* or Bchl*c* could have populations of macrocycles in which acetyl C=O and $CH_3CH(OH)$— are directly coordinated to Mg or hydrogen-bonded to Mg-coordinated water. Since Bchl*c* formed cylindrical micelles even when dried by techniques that assure the absence of water in other chlorophylls, it seems likely that the lattice of these dried micelles is formed by chains with Mg–$OHCHCH_3$ interactions (22, 23). Such chains are only possible in chlorophylls that lack a carbomethoxy group in ring V. Hydrogen bonding between the free hydrogen atom of the Mg-coordinated hydroxyl group and the keto C=O functions in another chain could then generate a two-dimensional lattice.

The mass/unit length (Table 1) of the Bchl*a* micelle is much larger than for the Chl*a* and Bchl*c* micelles. This is in part due to the larger radius of the Bchl*a* micelles, but also the surface of these micelles is more nearly a bilayer of macrocycles. The presence of two strong donor groups and the ability of the Mg acceptor to assume a coordination number of 6 can generate three-dimensional Bchl*a* structures by the interaction of acetyl C=O groups in one sheet with Mg atoms in another.

From the Fourier–Bessel transforms of Fig. 1, it is evident that the long aliphatic alcohols are arranged differently in micelles of the different chlorophylls. The narrowest scattering density profile is found for the P740 micelle and indicates that the phytyl groups must be on only one side of the cylinder. The profile for Bchl*c* micelles is significantly wider, even though the farnesyl esterifying alcohol is five carbon atoms shorter than the phytyl chains of Chl*a*. Thus, for Bchl*a* and -*c*, the esterifying moieties are on both the exterior and interior surfaces of the micelles. The molecular packing in the ethylchlorophyllide a·$2H_2O$ structure indicates that the phytyl chains can be located only on the outside of the Chl*a* cylinder, and the scattering density profile is consistent with this arrangement. Because Bchl*c* lacks the carbomethoxy group present in Chl*a* and Bchl*a*, the Bchl*c* macrocycles can be inserted into the lattice with a water molecule on either face of the macrocycle, which would result in farnesyl groups on both the interior and exterior surfaces of the cylinders.

Reticulated Models for Chlorophyll *in Vivo*. Bchl*c* cylindrical micelles provide a remarkably satisfactory model for the bulk chlorophyll in green photosynthetic bacteria (*Chlorobiaceae*). Freeze–fracture electron micrographs (24) show that chlorosomes (the hydrophobic organelles that contain the

Bchl*c*) of *Chlorobium limicola* forma sp. *thiosulfatophilum* contain "10–30 rod elements ≈10 nm in diameter." Our Bchl*c* micelles are about 11 nm in diameter (Table 1) and absorb light maximally at 750 nm, as does *C. limicola* (25). In a model proposed by Olson (26), the chlorosome rods are formed of protein subunits and the Bchl*c* occupies the central core and the spaces between subunits on the outer surface. As a result of our findings, we propose that a Bchl*c* lattice constitutes most of the surface of the rods and that the protein is interior to this lattice but associated to it. From the literature estimates, there is enough Bchl*c* to form at least 60–70% and possibly all of the rod surface (26), but some protein and/or lattice vacancies could also be present.

Features of the Bchl*a* cylindrical micelles, especially the curved chains of interacting macrocycles, also provide good models for the long-wavelength antenna chlorophyll in purple photosynthetic bacteria. The Bchl*a* micelles absorb maximally at 865 nm, with tailing out to 1000 nm, similar to the red-shift in these bacteria. The diameters of curvature are sufficient to enclose large proteins, such as reaction-center protein. Whether protein is interior to curved chains, either long or short, or whether two-dimensional networks are attached in reticulated patches that follow the contours of the protein cannot yet be decided. The photosynthetic membrane could limit the phytyl groups to one orientation, more like in interfacial monolayers than in our Bchl*a* cylinders, thus reducing the number of possible linkages. A role for the Bchl*a* micellar structures in special pair function can also be visualized, since symmetric pairs can be part of a chain of bacteriochlorophylls. An interesting aspect of a symmetric pair in a chain is that the curvature is changed to an "S" shape that could then link more than one protein. All of these possibilities now need to be explored.

A chlorophyll species absorbing at 740 nm is not a major natural component of green plants but is present to some extent in cyanobacteria (27). Treatment of green plant chloroplasts with 65% aqueous methanol converts the natural 680 nm absorption peak to 740 nm (28), which exactly parallels the optical changes when Chl*a* oligomers in octane solution are converted by addition of water to P740 micelles. It is possible, therefore, that in organisms containing Chl*a* as their sole chlorophyll, most of the Chl*a* occurs as water-free oligomers, $(\text{Chl}a)_n$ (6), that are the precursors of the P740 species formed by hydration. In green plants containing both Chl*a* and Chl*b*, the likely precursor is a mixed oligomer of the two chlorophylls, since mixtures of Chl*a* and -*b* are known to form micelles absorbing at 740 nm upon hydration.

The models we describe here account for the optical properties of bacterial antenna chlorophyll and are well-suited for light-harvesting purposes because of their curved yet quasicrystalline structures. The results make it possible to think about the organization of chlorophyll in photosynthetic organisms in more concrete terms and may make it possible to achieve a better understanding of the ways in which chlorophyll interacts with itself and the other components of the photosynthetic apparatus, and of how these interactions are involved in chlorophyll function in photosynthesis.

This work was performed under the auspices of the Office of Basic Energy Sciences, Division of Chemical Sciences, U.S. Department of Energy, under Contract W-31-109-ENG-38.

1. Clayton, R. K. (1965) *Molecular Physics in Photosynthesis* (Blaisdell, New York), p. 151.
2. Katz, J. J., Norris, J. R., Thurnauer, M. C. & Wasielewski, M. R. (1978) *Annu. Rev. Biophys. Bioeng.* **7,** 393–434.
3. Katz, J. J., Oettmeier, W. & Norris, J. R. (1976) *Philos. Trans. R. Soc. London Ser. B* **273,** 227–253.
4. Svec, W. A. (1978) in *The Porphyrins*, ed. Dolphin, D. (Academic, New York), Vol. 5, pp. 341–399.
5. Schaber, P. M., Hunt, J. E., Fries, R. & Katz, J. J. (1984) *J. Chromatogr.* **316,** 25–41.
6. Katz, J. J., Shipman, L. L., Cotton, T. M. & Janson, T. R. (1978) in *The Porphyrins*, ed. Dolphin, D. (Academic, New York), Vol. 5, pp. 401–458.
7. Stein, R. S. & Han, C. S. (1985) *Phys. Today* **38,** 74–80.
8. Chow, H.-C., Serlin, R. & Strouse, C. E. (1975) *J. Am. Chem. Soc.* **97,** 7230–7237.
9. Donnay, G. (1959) *Arch. Biochem. Biophys.* **80,** 80–85.
10. Jacobs, E. E., Vatter, A. E. & Holt, A. S. (1954) *Arch. Biochem. Biophys.* **53,** 228–238.
11. Flaumenhaft, E. & Katz, J. J. (1973) *J. Inorg. Nucl. Chem.* **35,** 1719–1725.
12. Serlin, R., Chow, H.-C. & Strouse, C. E. (1975) *J. Am. Chem. Soc.* **97,** 7237–7242.
13. Shipman, L. L., Norris, J. R. & Katz, J. J. (1976) *J. Phys. Chem.* **80,** 877–882.
14. Fischer, M. S., Templeton, D. H., Zalkin, A. & Calvin, M. (1971) *J. Am. Chem. Soc.* **94,** 3613–3619.
15. Hoppe, W., Will, G., Gassmann, J. & Weichselgartner, H. (1969) *Z. Kristallogr.* **128,** 18–35.
16. Barkigia, K. M., Fajer, J., Smith, K. M. & Williams, G. J. B. (1981) *J. Am. Chem. Soc.* **103,** 5890–5893.
17. Kratky, C. & Dunitz, J. D. (1977) *J. Mol. Biol.* **113,** 431–442.
18. Kratky, C., Isenring, H. P. & Dunitz, J. D. (1977) *Acta Crystallogr. B* **33,** 547–549.
19. Kratky, C. & Dunitz, J. D. (1975) *Acta Crystallogr. B* **31,** 1586–1589.
20. Fischer, M. S., Templeton, D. H., Zalkin, A. & Calvin, M. (1971) *J. Am. Chem. Soc.* **93,** 2622–2628.
21. Worcester, D. L. (1978) *Proc. Natl. Acad. Sci. USA* **75,** 5475–5477.
22. Bystrova, M. I., Mal'gosheva, I. N. & Krasnovskii, A. A. (1979) *Mol. Biol. (Engl. Transl.)* **13,** 440–451.
23. Smith, K. M., Kehres, L. A. & Fajer, J. (1983) *J. Am. Chem. Soc.* **105,** 1387–1389.
24. Stehlin, L. A., Golecki, J. R. & Drews, G. (1980) *Biochim. Biophys. Acta* **589,** 30–45.
25. Cruden, D. L. & Stanier, R. Y. (1970) *Arch. Microbiol.* **72,** 115–134.
26. Olson, J. M. (1980) *Biochim. Biophys. Acta* **594,** 33–51.
27. Govindjee (1961) *Science* **134,** 391–392.
28. Lippincott, J. A., Aghion, J., Porcile, E. & Bertsch, W. (1962) *Arch. Biochem. Biophys.* **98,** 17–27.